We are IntechOpen, the world's leading publisher of Open Access books Built by scientists, for scientists

4,800
Open access books available

122,000
International authors and editors

135M
Downloads

Our authors are among the

154
Countries delivered to

TOP 1%
most cited scientists

12.2%
Contributors from top 500 universities

WEB OF SCIENCE™

Selection of our books indexed in the Book Citation Index in Web of Science™ Core Collection (BKCI)

Interested in publishing with us?
Contact book.department@intechopen.com

Numbers displayed above are based on latest data collected.
For more information visit www.intechopen.com

7

Determination of Rotor Imbalances

Jenny Niebsch
Radon Institute of Computational and Applied Mathematics, Austrian Academy of Sciences
Austria

1. Introduction

During operation, rotor imbalances in wind energy converters (WEC) induce a centrifugal force, which is harmonic with respect to the rotating frequency and has an absolute value proportional to the square of the frequency. Imbalance driven forces cause vibrations of the entire WEC. The amplitude of the vibration also depends on the rotating frequency. If it is close to the bending eigenfrequency of the WEC, the vibration amplitudes increase and might even be visible. With the growing size of new WEC, the structure has become more flexible. As a side effect of this higher flexibility it might be necessary to pass through the critical speed in order to reach the operating frequency, which leads to strong vibrations. However, even if the operating frequency is not close to the eigenfrequency, the load from the imbalance still affects the drive train and might cause damage or early fatigue on other components, e.g., in the gear unit. This is one possible reason why in most cases the expected problem-free lifetime of a WEC of 20 years is not achieved. Therefore, reducing vibrations by removing imbalances is getting more and more attention within the WEC community.

Present methods to detect imbalances are mainly based on the processing of measured vibration data. In practice, a Condition Monitoring System (CMS) records the development of the vibration amplitude of the so called 1p vibration, which vibrates at the operating frequency. It generates an alarm if a pre-defined threshold is exceeded. In (Caselitz & Giebhardt, 2005), more advanced signal processing methods were developed and a trend analysis to generate an alarm system was presented. Although signal analysis can detect the presence of imbalances, the task of identify its position and magnitude remains.

Another critical case arises when different types of imbalances interfere. The two main types of rotor imbalances are mass and aerodynamic imbalances. A mass imbalance occurs if the center of gravitation does not coincides with the center of the hub. This can be due to various factors, e.g., different mass distributions in the blades that can originate in production inaccuracies, or the inclusion of water in one or more blades. Mass imbalances mainly cause vibrations in radial direction, i.e., within the rotor plane, but also smaller torsional vibrations since the rotor has a certain distance from the tower center, acting as a lever for the centrifugal force. Aerodynamic imbalances reflect different aerodynamic behavior of the blades. As a consequence the wind attacks each blade with different force and moments. This also results in vibrations and displacements of the WEC, here mainly in axial and torsional direction, but also in contributions to radial vibrations. There are multiple causes for aerodynamic imbalances, e.g., errors in the pitch angles or profile changes of the blades. The major differences in the impact of mass and aerodynamic imbalances are the main directions of the induced vibrations and the fact that aerodynamic imbalance loads change with the

wind velocity. Nevertheless, if the presence of aerodynamic imbalances is neglected in the modeling procedure, the determination of the mass imbalance can be faulty, and in the worst case, balancing with the determined weights can even increase the mass imbalance. As a consequence, the methods to determine mass imbalance need to ensure the absence of aerodynamic imbalances first.

In the field, the balancing process of a WEC is done as follows. An on-site expert team measures the vibrations in the radial, axial and torsion directions. Large axial and torsion vibrations indicate aerodynamic imbalances. The surfaces of the blades are investigated and optical methods are used to detect pitch angle deviation. The procedure to determine the mass imbalance is started after the cause of the aerodynamic imbalance is removed. In this procedure, the amplitude of the radial vibration is measured at a fixed operational speed, typically not too far away from the bending eigenfrequency. Afterwards a test mass (usually a mass belt) is placed at a distinguished blade and the measurements are repeated. From the reference and the original run, the mass imbalance and its position can be derived. Altogether, this is a time consuming and personnel-intensive procedure.

In (Ramlau & Niebsch, 2009) a procedure was presented that reconstructed a mass imbalance from vibration measurements without using test masses. The main idea in this approach is to replace the reference run by a mathematical model of the WEC. At this stage, only mass imbalances were considered. A simultaneous investigation of mass and aerodynamic imbalances was investigated by Borg and Kirchdorf, (Borg & Kirchhoff, 1998). The contribution of mass and aerodynamic imbalances to the 1p, 2p and 3p vibration was examined using a perturbation analysis in order to solve the differential equation that coupled the azimuth and yaw motion. Using the example of an NREL 15 kW turbine, the presence of 60 % mass imbalance and 40% aerodynamic imbalance explained by a 1 degree pitch angle deviation was observed. In (Nguyen, 2010) and (Niebsch et al., 2010) the model based determination of imbalances was expanded to the case of the presence of both mass imbalances and pitch angle deviation.

The main aim of this chapter is the presentation of a mathematical theory that allows the determination of mass and aerodynamical imbalances from vibrational measurements only. This task forms a typical inverse problem, i.e., we want to reconstruct the cause of a measured observation. In many cases, inverse problems are ill posed, which means that the solution of the problem does not depend continuously on the measured data, is not unique or does not exist at all. One consequence of ill-posedness is that small measurement errors might cause large deviations in the reconstruction. In order to stabilize the reconstruction, regularization methods have to be used, see Section 3.

Finding the solution of the inverse problem requires a good forward model, i.e., a model that computes the vibration of the WEC for a given imbalance distribution. This is realized by a structural model of the WEC, see Section 2. The determination of mass imbalances is briefly explained in Section 4. The mathematical description of loads from pitch angle deviations is considered in the same section as well. Section 5 presents the basic principle of the combined reconstruction of mass and aerodynamic imbalances.

2. Structural model of a wind turbine

2.1 The mathematical model

A structural dynamical model of an object or machine allows to predict the behavior of that object subjected to dynamic loads. There is a large variety of literature as well as software addressing this topic. Here, we followed the book (Gasch & Knothe, 1989), where the WEC

tower is modeled as a flexible beam, the rotor and nacelle are treated as point masses. The computation of displacements from dynamic loads can be described by a partial differential equation (PDE) or an equivalent energy formulation. Usually, both formulations do not result in an analytical solution. Using Finite Element Methods (FEM), the energy formulation can be transformed into a system of ordinary differential equations (ODE). The object, in our case the wind turbine, has to be divided into elements, here beam elements, with nodes at each end of an element, see Figure 1. The displacement of an arbitrary point of the element is approximated by a combination of the displacements of the start and the end node. The ODE system connecting dynamical loads and object displacements has the form

$$M\mathbf{u}''(t) + S\mathbf{u}(t) = \mathbf{p}(t). \tag{1}$$

Here, t denotes the time. The displacements are combined in the vector $\mathbf{u}$, which contains the degrees of freedom (DOF) of each node in our FE model. The degrees of freedom in each node can be the displacement (u, v, w) in all three space directions as well as torsion around the x-axis and cross sections slopes in the (x, y)- and (x, z)-plane: $(u, v, w, \beta_x, \beta_y, \beta_z)$, cf. Figure 2. The physical properties of our object are represented by the mass matrix M and the stiffness matrix S. The load vector $\mathbf{p}$ contains the dynamic load in each node arising from forces and moments. For this calculation, damping is neglected. Otherwise the term $D\mathbf{u}'$ with damping matrix D adds to the left hand side of equation (1). Considering mass imbalances

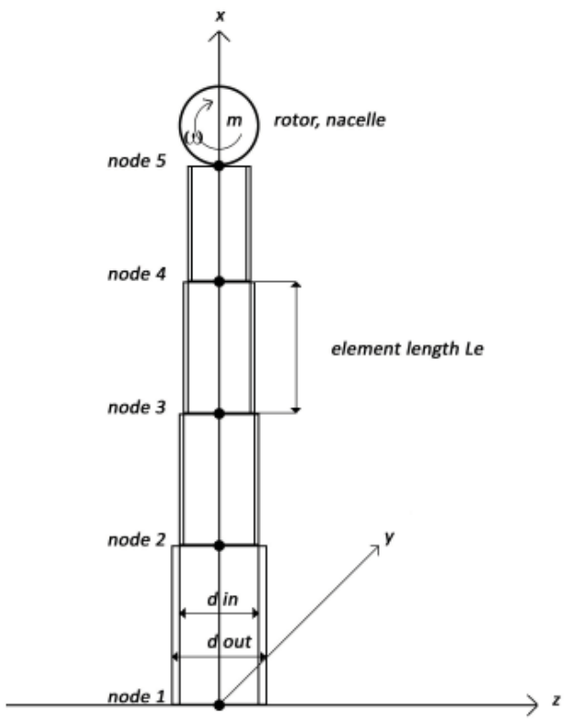

Fig. 1. Elements in a Finite Element model of a WEC

only, the forces and moments mainly act in radial direction, i.e., along the z-axis, and result in displacements and cross section slopes in that direction. Therefore, for each node we only consider the DOF (w, β_z). In order to construct the mass and the stiffness matrix each element

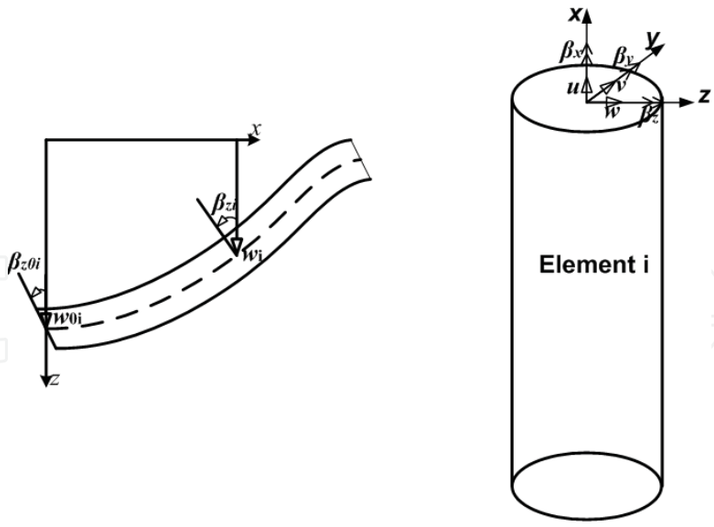

Fig. 2. Degrees of freedom in a Finite Element model of a WEC

is treated separately. The DOF of the bottom and the top node of the ith element are collected in the element DOF vector, cf. Figure 2,

$$\mathbf{u}_e^i = [w_{0i} \;\; \beta_{z0i} \;\; w_i \;\; \beta_{zi}]^T. \tag{2}$$

The derivation of the element mass and stiffness matrix M_e and S_e uses four shape functions scaled by the DOF of the bottom and top node to describe the DOF $(w_i(x), \beta_{zi}(x))$ of an arbitrary point x of the element. It is given in detail in (Gasch & Knothe, 1989). We only want to present the final formulas for the element matrices,

$$M_e = \frac{\mu L_e}{420} \begin{pmatrix} 156 & -22L_e & 54 & 13L_e \\ -22L_e & 4L_e^2 & -13L_e & -3L_e^2 \\ 54 & -13L_e & 156 & 22L_e \\ 13L_e & -3L_e^2 & 22L_e & 4L_e^2 \end{pmatrix}, \quad S_e = \frac{E \cdot I}{L_e^3} \begin{pmatrix} 12 & -6L_e & -12 & -6L_e \\ -6L_e & 4L_e^2 & 6L_e & 2L_e^2 \\ -12 & 6L_e & 12 & 6L_e \\ -6L_e & 2L_e^2 & 6L_e & 4L_e^2 \end{pmatrix}. \tag{3}$$

The length of the element is represented by L_e. E is Young's modulus, which is a material constant that can be found in a table . We assume our elements to be circular beam sections. The transverse moment of inertia I is given by $I = \pi/64 \cdot (d_{e,out}^4 - d_{e,in}^4)$ with outer and inner diameter of the beams section. μ is the translatorial mass per length $\mu = \varrho \cdot A$, where ϱ is the density of the material. $A = \pi/4 \cdot (d_{e,out}^2 - d_{e,in}^2)$ is the annulus area. To build the full system matrices S and M, the element matrices S_e and M_e are combined by superimposing the elements affecting the upper node of the ith element matrix with the ones belonging to the lower node of the $(i+1)$st element matrix, see Figure 3. The sum of rotor mass and nacelle mass m needs to be added to the last but one diagonal element of the full mass matrix. As mentioned above, the described model is restricted to radial displacements that are induced by radial forces, e.g., from mass imbalances. If we consider other types of load, e.g., aerodynamic, we have to deal with forces and moments in all three space directions. The derivation of the corresponding mass and stiffness matrix is a bit more comprehensive. In a general and abbreviated form it is given in (Gasch & Knothe, 1989). The application for a WEC is presented in Niebsch et al. (2010), and in a more detailed version in (Nguyen, 2010).

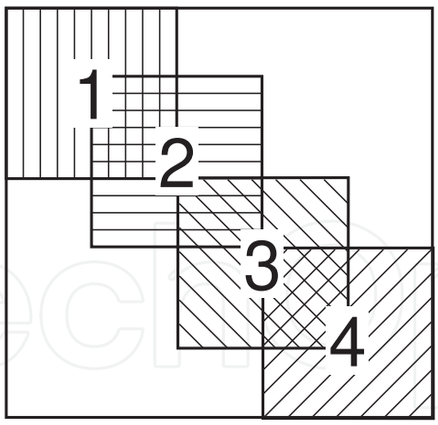

Fig. 3. System matrix and superimposed element matrices

2.2 Model optimization

Once M and S are determined, the solution of equation (1) for a given load $\mathbf{p}$ provides the displacement of each node in our model. We remark that the FEM is an approximative method. Additionally, the idealization of WEC as a flexible beam with a point mass as well as slight deviations in the geometric and physical parameters lead to model that approximates the reality but can not reproduce it exactly. Hence the system properties of our model, described by M and S, might differ slightly from the properties of the real WEC. In order to calibrate the model to the real WEC we have to chose one or more parameters that can be measured at the real WEC and then optimize our model according to those parameters. For our application the most important parameter of a WEC is the first (bending) eigenfrequency of the system. For each WEC type a range for the first eigenfrequency is given by the manufacturer, e.g., a VESTAS V80 of 100 m height has an eigenfrequency in the range $[0.21, \cdots, 0.255]$Hz. The actual eigenfrequency of a specific WEC of any type depends, e.g., on the grounding of the WEC and manufacturing tolerances in geometry and material. The eigenfrequency can be obtained from measurements during the performance of an emergency stop of the WEC. Thus our model, i.e., the matrices M and S, derived for a certain type of WEC from given geometrical and physical parameters as described above, can be optimized for specific WECs of that type with respect to the measured first eigenfrequency. The first eigenfrequency of the model can be computed using the assumption $\mathbf{u}(t) = \mathbf{u_0} \exp(\lambda t)$ and inserting it in the homogenous form of (1). Then we have to solve

$$\lambda^2 I \mathbf{u_0} = -M^{-1} S \mathbf{u_0} \,, \tag{4}$$

i.e., λ^2 are the eigenvalues of the matrix $-M^{-1}S$. For example, they can be obtained with the Matlab function *eig*. The eigenvalues are complex numbers. In the absence of damping, as in our case, the real part vanishes. The eigenfrequencies ω_{eig} are given by the imaginary part:

$$\omega_{eig} = \pm \Im \left(\sqrt{-eig(M^{-1}S)} \right). \tag{5}$$

The rotational first eigenfrequency is then given by

$$\Omega_0 = \frac{\min\{\omega_{eig}\}}{2\pi}. \tag{6}$$

Usually there is no information of the foundation and grounding available whereas manufacturing tolerances in the geometry, i.e., the length and the inner and outer diameter of the beam elements are accessible in the modeling process. In fact, Ω_0 is a function of those parameters. We can chose the geometric parameters from realistic intervals of manufacturing tolerances in such a way that the new model eigenfrequency is very close to the measured one. Supposing Ω is the measured first eigenfrequency of the WEC, the optimal geometric parameters can be found by minimizing the functional

$$\min_{\mathbf{L},\mathbf{d}_{in},\mathbf{d}_{out}} |\Omega - \Omega_0(\mathbf{L}, \mathbf{d}_{in}, \mathbf{d}_{out})|, \tag{7}$$

where the vectors $\mathbf{L}, \mathbf{d}_{in}, \mathbf{d}_{out}$ contain the length, inner and outer diameter of each element.

3. Introduction to inverse problems

Within this Section, we would like to introduce some basic concepts from the theory of inverse and ill posed problems. We will focus in particular on regularization theory, which has been extensively developed over the last decades. As we will see, regularization is always needed when the solution of a problem does not depend continuously on the data, which causes in particular problems if the data originate from (noisy) measurements. For details, we refer to (Engl et al., 2000).

We assume that the connection of two terms f and g such as an imbalance and the displacements resulting from that imbalance, is described by an operator $\mathbf{A}$:

$$\mathbf{A}f = g. \tag{8}$$

The computation of g for given f is called the forward problem while the determination of f for given g is referred to as the inverse problem. In practical applications the exact data g are not known but a measured noisy version g^δ of that data. We assume that the noise level is bounded by an unknown number δ, i.e.,

$$\|g - g^\delta\| \leq \delta. \tag{9}$$

The computation of an imbalance from vibration/displacement data is an inverse problem.

If the following three conditions are fulfilled, the Inverse Problem is called **well posed**:

1. For all data g there exists a solution f.
2. The solution f is unique.
3. The solution f depends continuously on the data g. ($\mathbf{A}^{-1}$ is continuous.)

The last condition ensures that small changes in the data g result in small changes in the solution f. A well posed inverse problem can be solved by applying the inverse operator to the data:

$$f = \mathbf{A}^{-1}g. \tag{10}$$

If one of the conditions is violated the inverse problem is called **ill posed**.

The violation of condition 1 can be fixed by the definition of a generalized solution. We compute our solution as the least-squares solution taking f as the element that minimizes the distance of $\mathbf{A}f$ to the data g:

$$f^\dagger = arg\min_f \|\mathbf{A}f - g\|^2. \tag{11}$$

The operator that maps the data g to the least-squares solution $f^\dagger$ is denoted by $\mathbf{A}^\dagger$ and called generalized inverse of $\mathbf{A}$. The violation of condition 2 can be rectified by distinguishing one solution from the set of all solutions. It can be the solution with the smallest norm or the one that best fits prior known properties of the desired solution.
In condition 3 we have to deal with the discontinuous inverse or generalized inverse operator. Small errors in the data can result in huge errors in the solution. To avoid this behavior, the discontinuous inverse is approximated pointwise by a family of continuous operators. To be more precise, we have to find a family of operators $\mathbf{T}_\alpha$, with a regularization parameter $\alpha = \alpha(\delta, g^\delta)$, that fulfills the conditions

$$\alpha(\delta) \xrightarrow{\delta \to 0} 0, \quad \lim_{\delta \to 0} \mathbf{T}_\alpha g^\delta = \mathbf{A}^\dagger g. \tag{12}$$

This implies that for very small data error δ the parameter α becomes small and the corresponding continuous $\mathbf{T}_\alpha$ is a good approximation to $\mathbf{A}^\dagger$. The right choice of α is difficult because the error we get by computing $f_\alpha^\delta = \mathbf{T}_\alpha g^\delta$ as an approximate solution of $f^\dagger = \mathbf{A}^\dagger g$ has two parts that behave very differently:

$$\|\mathbf{T}_\alpha g^\delta - \mathbf{A}^\dagger g\| \leq \underbrace{\|\mathbf{T}_\alpha g^\delta - \mathbf{T}_\alpha g\|}_{\textit{propagated data error}} + \underbrace{\|\mathbf{T}_\alpha g - \mathbf{A}^\dagger g\|}_{\textit{approximation error}}. \tag{13}$$

The approximation error decreases with α while the propagated data error increases with decreasing α, cf. Figure 4. This is due to the fact that for small α the operator $\mathbf{T}_\alpha$ is closer to $\mathbf{A}^\dagger$ and thus "less continuous" than for bigger α. The total error has a minimum away from $\alpha = 0$. To find the parameter α with minimal error $\|\mathbf{T}_\alpha g^\delta - \mathbf{A}^\dagger g\|$, a parameter choice rule is necessary. The operator family defined in (12) combined with a parameter choice rule is called **regularization method**.
A widely used example for a regularization method is Tikhonov's regularization where the operator $\mathbf{T}_\alpha$ is given by

$$\mathbf{T}_\alpha = (\mathbf{A}^*\mathbf{A} + \alpha\mathbf{I})^{-1}\mathbf{A}^*, \tag{14}$$

where $\mathbf{I}$ is the identity and $\mathbf{A}^*$ denotes the adjoint operator of $\mathbf{A}$. In case $\mathbf{A}$ is a matrix, $\mathbf{A}^*$ is the transpose of $\mathbf{A}$. Alternatively, $f_\alpha^\delta = \mathbf{T}_\alpha g^\delta$ can be characterized as the unique minimizer of the Tikhonov functional

$$J_\alpha(f) = \|\mathbf{A}f - g^\delta\|^2 + \alpha\|f\|^2. \tag{15}$$

The characterization of f_α^δ via the Tikhonov functional is in particular important as it allows a straightforward generalization for nonlinear operators. The linear operator can simply be replaced by a nonlinear operator. We mention this because the consideration of aerodynamic imbalances leads to a nonlinear operator $\mathbf{A}$. The determination of the regularization parameter α depends on properties of the operator and the choice of the regularization method, (Engl et al., 2000). In principle, there are a-priori parameter choice rules, where α can be determined from prior information, and a-posteriori rules. A well known a posteriori parameter choice rule is Morozov's discrepancy principle where α is chosen s.t.

$$\delta \leq \|g^\delta - \mathbf{A}f_\alpha^\delta\|^2 \leq c\delta \tag{16}$$

holds (Morozov, 1984). The application of the discrepancy principle requires the computation of the approximate solution f_α^δ for a chosen α first. Afterwards (16) is checked and α has to be

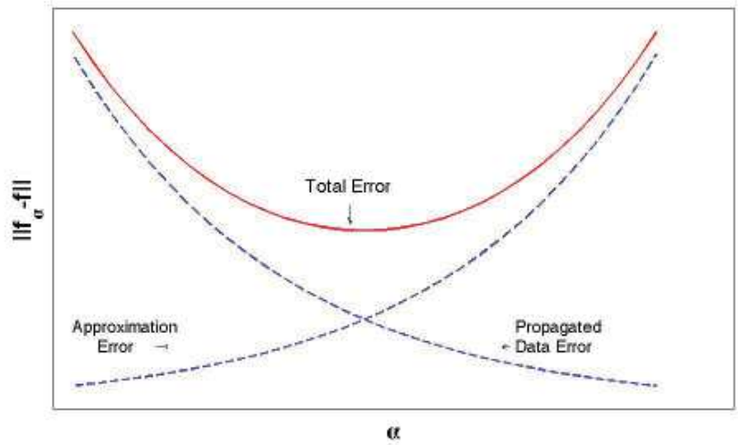

Fig. 4. Regularization error

changed if the condition does not hold. All a-posteriori parameter choice rules depend on the data error level δ and the data g^δ. Very popular are heuristic parameter choice rules, where the regularization parameter is independent of the noise level δ. Examples are the L-curve method (Hansen P., 1992) or the quasi-optimality rule (Kindermann, 2008). Please note that heuristic parameter choice rules do not lead to convergent regularization methods, although they perform well in many applications.

4. Imbalance determination

The determination of imbalances from measurements of the induced vibrations (or displacements) is an inverse problem as explained above.

4.1 Mass imbalance

First, we restrict ourself to the determination of mass imbalances and assume that aerodynamic imbalances are insignificant. In the structural model section we mentioned that in this case we only need a model that considers DOF in radial or z-direction. The knowledge of the mass and stiffness matrix provides us with a connection of the loads from imbalances $\mathbf{p}$ and the resulting displacements $\mathbf{u}$ in the nodes of our model via equation (1).
A mass imbalance can be described by a mass m that is located at a distance r from the rotor center and has an angle φ to a certain zero mark of the rotor, usually blade A, cf. Figure 5. If the rotor revolves with revolutionary frequency Ω, the mass imbalance induces a centrifugal force of absolute value $\omega^2 mr$, with the angular velocity $\omega = 2\pi\Omega$. The force or load vector is given by:

$$p(t) = \omega^2 mre^{i(\omega t+\varphi)} =: p_0\omega^2 e^{i\omega t}, \tag{17}$$

where $p_0 = mre^{i\varphi}$ defines the mass imbalance in absolute value and phase location. Harmonic loads of the form (17) cause harmonic vibration $\mathbf{u} = \mathbf{u}_0 e^{i\omega t}$ of the same frequency ω. Inserting $\mathbf{u}$, its second derivative and $\mathbf{p} = \mathbf{p}_0 e^{i\omega t}$ into equation (1), time dependency cancels out and we get an explicit solution for the vibration amplitudes $\mathbf{u}_0$:

$$\mathbf{u}_0 = (-M + \omega^{-2}S)^{-1}\mathbf{p}_0. \tag{18}$$

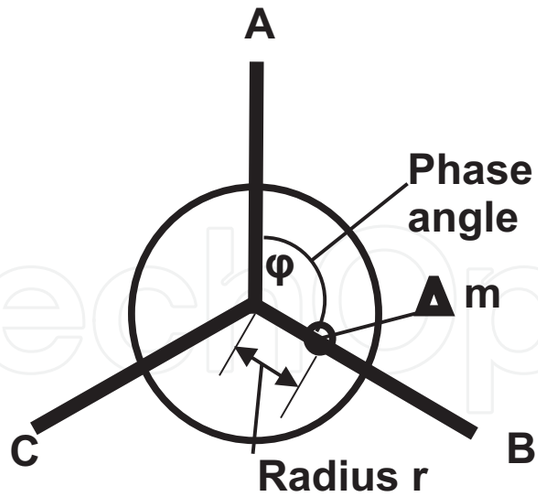

Fig. 5. Mass imbalance

The matrix $(-M+\omega^{-2}S)^{-1}$ would define our forward operator in (8) if we would assume that the vibration amplitudes could be measured in every node of the model. Usually this is not possible, measurements are taken in the nacelle which is represented by the last model node, cf. Figure 1. Additionally, the rotor and its load are located at that node, too. Thus the load vector $\mathbf{p}_0$ would have only one entry, p_0 from (17), at the last but one position that corresponds to the displacement DOF w of the last node. Hence in (8) now $f = p_0$, $g = u_0$ the displacement of the last node, and $\mathbf{A}$ is just the element in the last but one row and last but one column of $(-M+\omega^{-2}S)^{-1}$. Denoting the number of DOF by N we have

$$\mathbf{A}p_0 = u_0, \quad \mathbf{A} = (-M+\omega^{-2}S)^{-1}_{(N-1,N-1)}. \tag{19}$$

We remark that u_0 is the complex amplitude containing the absolute value and the phase angle $u_0 = u_a e^{i\phi}$.
The measured values for u_a and ϕ are denoted by u_a^δ and ϕ^δ. Since $\mathbf{A}$ is a complex number we deal with the simplest well posed inverse problem possible. It is solved by

$$p_0^\delta = \frac{1}{\mathbf{A}} u_0^\delta. \tag{20}$$

4.2 Aerodynamic imbalance from pitch angle deviation

The main cause for aerodynamic imbalances is a deviation between the pitch angles of the blades, e.g., from assembling inaccuracies. Depending on the wind conditions, even a small deviation of one of the pitch angles can cause large forces and moments to be transferred onto the rotor. This results in displacements in direction of the rotor axis (the y-axis) as well as torsion around the tower axis (x-axis). But there are also forces in radial direction that add to the forces from mass imbalances and are not negligible. Hence, neglecting aerodynamic imbalances could result in an inaccurate determination of mass imbalances. In the worst case, the computed balancing mass and position could increase the mass imbalance. The mass imbalance estimation described in the former section can only be applied if aerodynamic imbalances are small enough. Currently, the WEC is checked for axial and torsional vibrations. If large corresponding amplitudes indicate an aerodynamic imbalance, the surfaces of the blades are checked and photographic measurements are carried out to find a possible pitch

angle deviation. After its correction the mass imbalance can be determined with the usual method.

The simultaneous reconstruction of mass and aerodynamic imbalances was considered in (Nguyen, 2010) and (Niebsch et al., 2010). The principle is the same as in the reconstruction of mass imbalances but now the structural model of the WEC is extended to DOF in radial and axial direction as well as torsion around the tower axis. Additionally, we have to describe the loads from aerodynamic imbalances mathematically. This was done using the Blade Element Momentum (BEM) theory, which is commonly used for simulations of WECs, see, e.g., (Hansen, 2008; Ingram, 2005). The result of the BEM theory are the tangential and normal (or thrust) force distributed over the blades that are divided into elements. The distributed forces are summed up to an equivalent normal force F_i with a distance l_i from the rotor center as well as an equivalent tangential force T_i, cf. Figure 6.

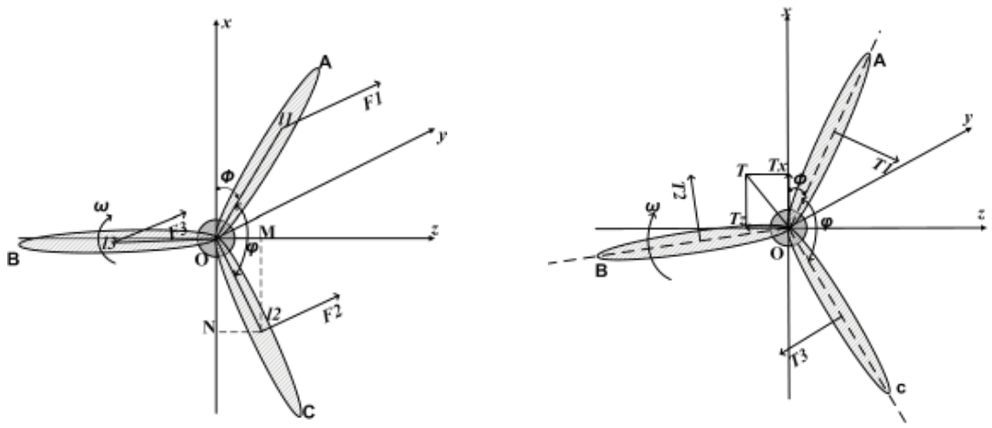

(a) Thrust forces F_i (b) Tangential forces T_i

Fig. 6. Normal (thrust) and tangential forces on the rotor blades

The forces depend on the pitch angle of the blade, the airfoil data, the angle of attack of the wind, and the relative wind velocity, as well as a lift and drag coefficient table. For details we refer to (Niebsch et al., 2010).

The force to the rotor in the axial (y-) direction is calculated by:

$$F_y = F_1 + F_2 + F_3. \tag{21}$$

The moments induced by this forces are given by

$$\begin{aligned} M_x^1 &= F_1 l_1 \sin(\omega t + \phi) + F_2 l_2 \sin(\omega t + \phi + \varphi) + F_3 l_3 \sin(\omega t + \phi + 2\varphi), \\ M_z^1 &= F_1 l_1 \cos(\omega t + \phi) + F_2 l_2 \cos(\omega t + \phi + \varphi) + F_3 l_3 \cos(\omega t + \phi + 2\varphi), \end{aligned} \tag{22}$$

where M_x^1 and M_z^1 denote the moments around the x- and the z-axis on the rotor and $\varphi = \frac{2\pi}{3} (\equiv 120^\circ)$ is the angle between the rotor blades. Note that if all blades have the same pitch angle, we have $F_1 = F_2 = F_3$ and $l_1 = l_2 = l_3$. This means that the moments M_x^1 and M_z^1 vanish. The projection of the total tangential force $T = T_1 + T_2 + T_3$ onto the z-axis and the x-axis is given by

$$\begin{aligned} T_z &= T_1 \cos(\omega t + \phi) + T_2 \cos(\omega t + \phi + \varphi) + T_3 \cos(\omega t + \phi + 2\varphi), \\ T_x &= T_1 \sin(\omega t + \phi) + T_2 \sin(\omega t + \phi + \varphi) + T_3 \sin(\omega t + \phi + 2\varphi). \end{aligned} \tag{23}$$

Since we have a small distance D between rotor plane and the tower center, T_z and T_x also produce moments around the x- and the z-axes:

$$M_x^2 = T_z \cdot D, \quad M_z^2 = T_x \cdot D. \tag{24}$$

With the formulas (21) - (24) we can describe the load vector $\mathbf{p}(t)$ in (1), which has only entries at the last node. We recall that the node has the DOF $(v, w, \beta_x, \beta_y, \beta_z)$, hence

$$\mathbf{p} = (0, \cdots, 0, F_y, F_z, M_x, M_y, M_z)^T, \tag{25}$$

with $F_z = T_z$, $M_x = M_x^1 + M_x^2$, and $M_z = M_z^1 + M_z^2$. We remark that M_y is converted into the rotational movement and finally into electrical energy. M_y should not add any contribution to the load vector.

5. Combination of mass and aerodynamic imbalances

The simultaneous consideration of mass and aerodynamic imbalances is also based on equation (1). As mentioned in the last section, for aerodynamic imbalances a model is required that includes DOF in the radial and axial directions as well as torsion around the tower axis. The combined presence of both imbalance types also requires a combination of the associated load vectors. We recall that the centrifugal force from a point mass imbalance is given by $\omega^2 mr$, the location of the eccentric mass is given by the radius r and the angle ϕ_m measured from a zero mark (blade A). The projections of the force onto the z- and x-axis are

$$\begin{aligned} F_z^2 &= \omega^2 mr \cos(\omega t + \phi + \phi_m), \\ F_x &= \omega^2 mr \sin(\omega t + \phi + \phi_m). \end{aligned} \tag{26}$$

Here, ϕ is the angle between blade A and the x-axis. Because the rotational plane has a distance D to the tower, the forces F_z^2 and F_x also produce moments around the x- and the z-axes:

$$\begin{aligned} M_x^3 &= F_z^2 \cdot D, \\ M_z^3 &= F_x \cdot D. \end{aligned} \tag{27}$$

The force in x-direction is of no consequence since we assume the tower to be rigid. But the moments M_x^3, M_z^3 and the force F_z^2 have to be added to the moments and forces from pitch angle deviation as described in (25). The forces and moments of the combined load vector add to

$$\begin{aligned} F_y &= F_1 + F_2 + F_3 \\ F_z &= T_z + F_z^2 \\ M_x &= M_x^1 + M_x^2 + M_x^3 \\ M_z &= M_z^1 + M_z^2 + M_z^3. \end{aligned} \tag{28}$$

We observe that the forces and moments in (28) are either constant (F_y) or harmonic. Therefore, equation (1) with a load vector of the form (25) and entries (28) can be solved explicitly. Details on the solution are given in (Niebsch et al., 2010).
Starting from the pitch angles of the three blades $(\theta_1, \theta_2, \theta_3)$, and from the characteristics of a mass imbalance (mr, ϕ_m) and assuming given values for angular speed $\omega = 2\pi\Omega$, wind

speed, and airfoil data, we have all the tools to determine the corresponding imbalance load $\mathbf{p}$ using the BEM method for the pitch angle deviation and by projecting (17) onto the x- and the z-axis. Solving (1) produces the resulting displacements $\mathbf{u}$. The restriction of the vector $\mathbf{u}$ onto the DOF that can be measures are denoted by $\mathbf{g} = \mathbf{u}_{|sensor}$. We combine all these operations into the forward operator $\mathbf{A}$:

$$\mathbf{A}(\theta_1, \theta_2, \theta_3, mr, \phi_m) = \mathbf{g}. \tag{29}$$

We remark that the BEM uses nonlinear optimization routines to compute parameter values in the equations for the normal and tangential force. Therefore, the final operator $\mathbf{A}$ is nonlinear. The vector $(\theta_1, \theta_2, \theta_3, mr, \phi_m)$ plays the role of f in (8). Usually, the radial and axial vibration, and the torsion around the tower axis are measurable using three acceleration sensors. Since the acceleration sensors do not measure the initial offset arising from the constant force F_y we have to rely on radial and torsion measurements only. For a known or estimated noise level δ of the measurements we can compute the solution $(\theta_1, \theta_2, \theta_3, mr, \phi_m)_\alpha^\delta$ as the minimizer of the Tikhonov functional (15). Since $\mathbf{A}$ is a nonlinear operator, minimization methods have to be employed to find the minimizing element, like e.g., the MATLAb implemented routines like *fminsearch* or gradient based methods. The regularization parameter α can be chosen iteratively using Morozov's Discrepancy Principle (16). First results on the simultaneous reconstruction of $(\theta_1, \theta_2, \theta_3, mr, \phi_m)$ from noisy data $\mathbf{g}^\delta$ were obtained in (Niebsch et al., 2010) with data errors of about 10%. Several experiments showed that the simultaneous reconstruction is successful provided we have a fairly good initial value for the mass imbalance. This can be obtained in a first step by reconstructing the mass imbalance neglecting pitch angle deviations with the method described in Section 4. The result is not the true mass imbalance but a sufficiently accurate initial estimate for the simultaneous reconstruction carried out as a second step. To present an example, a pitch angle deviation of 3 degree of the blade B as well as a mass imbalance of 350 kgm located at blade B. The data $\mathbf{g}$ were calculated by the forward computation of $\mathbf{A}(0°, 3°, 0°, 350\ kgm, 120°)$ and contaminated with 10% noise. The two step reconstruction from the noisy data resulted in $(-0.25°, 2.8°, 0.43°, 342\ \ kgm, 121°)$. The correction of the pitch angles and the setting of balancing weights according to that reconstruction lead to a significant reduction of the vibration, cf. Figure 7.

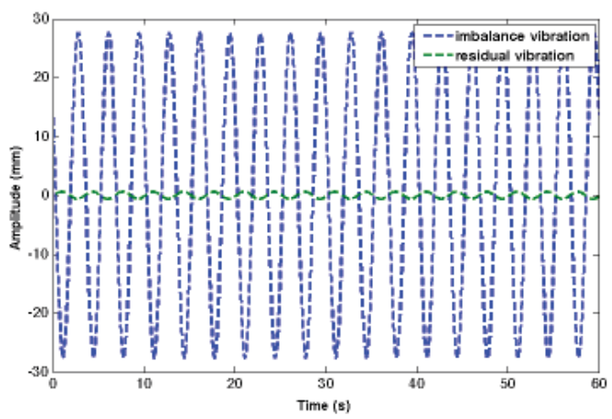

Fig. 7. Vibrations in z-direction before and after balancing

6. Conclusion

We presented a method to determine imbalances from vibration measurements based on a relatively simple model of the WEC under consideration. In contrast to detection methods based on signal processing, the imbalance can be localized and quantified. Moreover, mass imbalances and pitch angle deviations that cause aerodynamic imbalances can be discovered simultaneously. The model of the WEC is used to describe the connection of an imbalance load and the caused vibrations or displacements mathematically. The reverse direction of recovering an imbalance from given noisy vibration measurements is an inverse (ill-posed) problem and has to be treated accordingly. For this reason, we presented a short introduction to the main ideas and issues of the inverse problem theory.

In addition to the model parameters, the presented method requires the mathematical description of the loads from the different types of imbalances. Whereas for mass imbalances this is quite simple, the forces from pitch angle deviation are computed via the BEM method which uses idealizations that do not cover all effects that might arise during the operation of the WEC. Another drawback of the determination of pitch angle deviations is the fact that the BEM method requires the airfoil data of the WEC's blades. For most of the newer wind turbines this data are a well kept secret of the manufacturers. The restriction of the imbalance estimation to mass imbalances is much easier to implement into an existing condition monitoring system and does not require "sensitive" data.

We propose two main questions for future research. First, the assumption of a constant revolution frequency is not realistic. Therefore we have to consider equation (1) for a variable (time dependent) angular velocity ω, which allows the use of vibration data measured at variable speed. Presently, only data collected with constant or almost constant operational speed can be used for the imbalance determination. The second question is how to avoid the sensitive information on airfoil data that is necessary to reconstruct pitch angle deviations.

7. References

Borg, J. P. & Kirchhoff, R. H. (1998). Mass and Aerodynamic Imbalance of a Horizontal Axis Wind Turbine. *ASME Journal of Solar Energy Engineering* Vol. 120, 66-74.

Ciang, C. C., Lee, J., Bang, H. (2008). Structural health monitoring for a wind turbine system: a review of damage detection methods. *Meas.Sci.Technol.* , Vol. 19,122001(20pp).

Caselitz, P. & Giebhardt, J. (2005). Rotor Condition Monitoring for Improved Operational Safety of Offshore Wind Energy Converters. *ASME Journal of Solar Energy Engineering* Vol. 127, 253-261.

Engl, H. W..; Hanke, M. & Neubauer, A. (2000). *Regularization of Inverse Problems*, Kluwer, Dortrecht.

Gasch, R. & Knothe, K. (1989). *Strukturdynamik 2*, Springer, Berlin.

Hau, E. (2006). *Wind Turbines: Fundamentals, Technologies, Application, Economics*; Springer, Berlin, Heidelberg.

Hansen, M. (2008). *Aerodynamics of Wind Turbines*; Earthscan, London.

Hansen, P. C. (1992). Analysis of discrete ill-posed problems by means of the L-curve. *SIAM Rev*; Vol. 34 561-580.

Ingram, G. (2005). Wind Turbine Blade Analysis using the Blade Element Momentum Method. *Note on the BEM method*, Durham University, Durham.

Kindermann, S. & Neubauer, A. (2008) On the convergence of the quasi-optimality criterion for (iterated) Tikhonov regularization. *Inverse Problems and Imaging* Vol. 2, Nr. 2, 291-299.

Morozov, V. A. (1984). *Methods for Solving Incorrectly posed Problems*, Springer, New York, Berlin Heidelberg.

Niebsch, J.; Ramlau, R. & Nguyen, T. T. (2010). Mass and aerodynamic Imbalance Estimates of Wind Turbines. *Engergies*, Vol. 3, p 696-710, ISSN 1996-1073.

Nguyen, T. T. (2010). Mass and aerodynamic Imbalance Estimates of Wind Turbines. *Diploma thesis at the Johannes Kepler University Linz, Austria*.

Ramlau, R. (2002). Morozov's Discrepancy Principle for Tikhonov regularization of nonlinear operators. *Numerical Functional Analysis and Optimization*, Vol. 23 No.1&2, 147-172.

Ramlau, R. & Niebsch, J. (2009). Imbalance Estimation Without Test Masses for Wind Turbines. *ASME Journal of Solar Energy Engineering* Vol. 131, No. 1, 011010-1- 011010-7.

Scherzer, O. (1993). Morozov's Discrepancy Principle for Tikhonov regularization of nonlinear operators. *Computing*, Vol. 51 , 45-60.

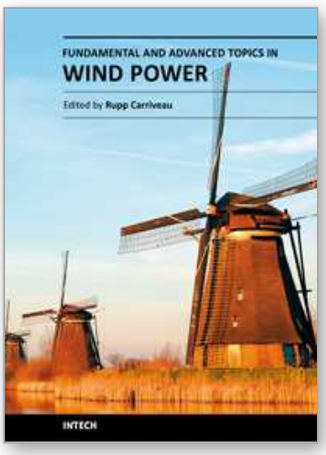

Fundamental and Advanced Topics in Wind Power
Edited by Dr. Rupp Carriveau

ISBN 978-953-307-508-2
Hard cover, 422 pages
Publisher InTech
Published online 20, June, 2011
Published in print edition June, 2011

As the fastest growing source of energy in the world, wind has a very important role to play in the global energy mix. This text covers a spectrum of leading edge topics critical to the rapidly evolving wind power industry. The reader is introduced to the fundamentals of wind energy aerodynamics; then essential structural, mechanical, and electrical subjects are discussed. The book is composed of three sections that include the Aerodynamics and Environmental Loading of Wind Turbines, Structural and Electromechanical Elements of Wind Power Conversion, and Wind Turbine Control and System Integration. In addition to the fundamental rudiments illustrated, the reader will be exposed to specialized applied and advanced topics including magnetic suspension bearing systems, structural health monitoring, and the optimized integration of wind power into micro and smart grids.

How to reference
In order to correctly reference this scholarly work, feel free to copy and paste the following:

Jenny Niebsch (2011). Determination of Rotor Imbalances, Fundamental and Advanced Topics in Wind Power, Dr. Rupp Carriveau (Ed.), ISBN: 978-953-307-508-2, InTech, Available from: http://www.intechopen.com/books/fundamental-and-advanced-topics-in-wind-power/determination-of-rotor-imbalances

INTECH
open science | open minds

InTech Europe
University Campus STeP Ri
Slavka Krautzeka 83/A
51000 Rijeka, Croatia
Phone: +385 (51) 770 447
Fax: +385 (51) 686 166
www.intechopen.com

InTech China
Unit 405, Office Block, Hotel Equatorial Shanghai
No.65, Yan An Road (West), Shanghai, 200040, China
中国上海市延安西路65号上海国际贵都大饭店办公楼405单元
Phone: +86-21-62489820
Fax: +86-21-62489821

IntechOpen